

Color Image Gradients for Morphological Segmentation

ROBERTO HIRATA JR.¹,
FRANKLIN CÉSAR FLORES¹,
JUNIOR BARRERA¹,
ROBERTO A. LOTUFO² AND
FERNAND MEYER³

¹ Instituto de Matemática e Estatística - USP
PO Box 66.281
05315-970 São Paulo - SP - Brazil
<hirata, fcflores, jb>@ime.usp.br

² Faculty of Electrical and Computer Engineering - UNICAMP
PO Box 6101
13081-970 Campinas - SP - Brazil
lotufo@dca.fee.unicamp.br

³ Centre de Morphologie Mathématique - École des Mines de Paris
35, rue St. Honore
77305 Fontainebleu - France
meyer@cmm.ensmp.fr

Abstract. This paper proposes an approach for color segmentation which is an alternative to the search of a total order in the color space. Instead of looking for a total order, we look for a suitable metric that defines a color gradient, which is a fundamental step of the morphological segmentation paradigm.

1 Introduction

An important step in morphological segmentation is to enhance the edges of the objects in the image to be segmented. After edge enhancement, the morphological segmentation paradigm can be applied. For grayscale images, the *Morphological Gradient* [1, 2] is a very good option. The result of this operator is a grayscale image, where each point is the difference between the maximum and the minimum graylevels of the image inside a structuring element (i.e., a finite subset of the domain). Therefore, the gradient operator enhances the differences between pixels inside the structuring element.

The detection of edges in color images is easier for the human eye, because there are much more dissimilarity information. However, the design of image processing tools to enhance edges in color images is much more complex. The natural dissimilarity measure in grayscale images is just the difference of intensities between pixels, while in color images a measure of the intuitive notion of the dissimilarity between colors is necessary. Unfortunately, such metric is unknown.

Even though the color space can be seen as a complete

lattice, the order relation is not total and if one imposes a total order, it will not be natural for the human eye. In other words, the human eye does not objectively compare two colors, for instance, red and blue, and decides which one is higher.

The main objective of this paper is not to look for a total order relation in the color space like other related works [3, 4], but to look for suitable metrics to compute a gradient for color images. We believe this approach is more sound because it does not impose any artificial order relation, but try to keep the intuitive notion of dissimilarity between colors.

Following this introduction, Section 2 presents color images and discusses the main problem related with the definition of color image operators. Section 3 presents several definitions of color gradients and their applicability. Section 4 reviews the morphological segmentation paradigm. Section 5 presents some comparisons between the defined gradients. Section 6 discusses some directions for future research.

The color images shown in this paper are available at our web site: <http://www.vision.ime.usp.br/demos>.

2 Color Images and Space Models

This section characterizes color images, recalls some color image models and discusses the root of the major problem related to color image operators definition.

Let L_1, L_2, \dots, L_m be totally ordered complete lattices (also called chains) [2]. For instance: a subset of \mathbf{Z} , or a closed subset of \mathbb{R} are chains. Let \vee denote the *supremum*, or maximum, and \wedge the *infimum*, or minimum, operations in chains. Let L be the Cartesian product of L_1, L_2, \dots, L_m , i.e., $l \in L \iff l = (l_1, l_2, \dots, l_m), l_i \in L_i, i = \{1, \dots, m\}$.

Let E be a non empty set that is an Abelian group with respect to a binary operation denoted by $+$. A mapping f from E to L , $f(z) = (f_1(z), f_2(z), \dots, f_m(z))$, $f_i : E \rightarrow L_i$ and $z \in E$ is called a *multivalued* or *multispectral* image. The mappings f_i are called *bands* of the image. A color image is an example of a multivalued function where $L = L_1 \times L_2 \times L_3$ is the representation of the colors under a certain color space model (a coordinate system where each point represents a unique color) [5, 6]. Let $\text{Fun}[E, L]$ denote the set of all mappings from E to L , i.e., all the possible color images.

Three different color space models are used in this paper: RGB (*Red, Green and Blue*), IHS (*Intensity, Hue and Saturation*) and YIQ (the usual N.T.S.C. transmission color coordinate systems).

The RGB system is a cube defined in a Cartesian system. This cube is defined by three subspaces related to one of the three primary colors, red, green and blue, and the pure representation of these colors are located at three corners of the cube. The other corners represent the inverse colors cyan, magenta and yellow, plus the white and black. Generally, one color is represented by a point inside this cube.

The IHS system is defined by a coordinate transformation of the RGB system [6]. This color space is composed by three attributes: *Intensity* (holds the luminosity information), *Hue* (describes uniquely a color in its pure form; for example, the red color without any information from other attributes) and *Saturation* (measures the amount of white light mixed with pure colors).

The YIQ system is used in the known N.T.S.C. color television standard. The Y value is the luminance of a color. The I and Q values jointly describe the hue and saturation attributes of a color.

From now on, let L_1, L_2 and L_3 be three generic chains and L be their Cartesian product. Let \prec be an order relation over L such that $l \prec l'$ if and only if each component of l' is greater than the correspondent component of l , i.e., $l \prec l' \iff (l_1 \leq l'_1, l_2 \leq l'_2, l_3 \leq l'_3)$, for any $l, l' \in L$.

The set L with the order relation \prec form a lattice structure [2]. The supremum (respec., infimum) of l and l' , $l \vee l'$ (respec. $l \wedge l'$), ($l, l' \in L$), is the supremum (respec., infimum)

of its components, i.e., $l \vee l' = (l_1 \vee l'_1, l_2 \vee l'_2, l_3 \vee l'_3)$ (respec., $l \wedge l' = (l_1 \wedge l'_1, l_2 \wedge l'_2, l_3 \wedge l'_3)$).

Even though L is a complete lattice, i.e., there exists an order relation between its elements, this order is not total. Some works in the literature [3, 4] imposes a total order to this lattice, but a total order here will not be natural in the sense that it will not reflect the correct perception of the human eye. However, when the order is not total, the supremum and infimum of two colors l and l' ($l, l' \in L$) may be neither l nor l' as is the case of a chain like the graylevel range. This is one of the problems with color image operators: extra colors can be created in the process of transforming a color image into another. For instance, the yellow color is the "supremum" between red and green ones.

For segmentation purposes, we use the color information for finding markers and enhance edges. To enhance edges we use suitable color metrics to define color gradients, which transforms the color image into a graylevel one.

3 Gradient Operators for Color Images

In this section we present several definitions of gradients for color images and a discussion of their applicability.

Let f be a color image, i.e., $f \in \text{Fun}[E, L]$, where $E \subset \mathbf{Z} \times \mathbf{Z}$ and $L = K \times K \times K$, if f is in the RGB or YIQ color models; or $L = K \times \Theta \times K$, if f is in the IHS color model ($K = [0, 1, 2, 3, \dots, k-1]$ and $\Theta = [0, 359]$).

Let $x \in E$. The translation of $B \subset E$ by x , denoted B_x , is given by $B_x = \{y \in E : (y - x) \in B\}$.

The following operator definitions are morphological gradients.

Definition 3.1 Given $g \in \text{Fun}[E, K]$, the gradient of g , $\nabla_B(g)$, is given by:

$$\nabla_B(g) = \delta_B(g) - \varepsilon_B(g), \quad (1)$$

where δ and ε are, respectively, the morphological dilation and erosion [1, 2], and $B \subset E$ is the structuring element of those operators.

The result of these operators is an image where each point is the maximum difference of graylevel inside B .

Definition 3.2 Given $g \in \text{Fun}[E, K]$, the internal gradient of g , $\nabla_B^i(g)$, is given by:

$$\nabla_B^i(g) = g - \varepsilon_B(g), \quad (2)$$

where ε is the morphological erosion and $B \subset E$ is a structuring element.

These two definitions make it possible to define two color gradients.

Definition 3.3 Given $f \in Fun[E, L]$, the color gradient I of f , $\nabla_B^I(f)$, is given by:

$$\nabla_B^I(f) = \bigvee \{\nabla_B(f_1), \nabla_B(f_2), \nabla_B(f_3)\}, \quad (3)$$

where $\nabla_B(\bullet)$ is the morphological gradient and $B \subset E$ is a structuring element.

The result of this color gradient is a graylevel image where each point is the maximum of the maximum difference of graylevel in B for each band of the color image.

Definition 3.4 Given $f \in Fun[E, L]$, the color gradient II of f , $\nabla_B^{II}(f)$, is given by:

$$\nabla_B^{II}(f) = \bigvee \{\nabla_B^i(f_1), \nabla_B^i(f_2), \nabla_B^i(f_3)\}, \quad (4)$$

where $\nabla_B^i(\bullet)$ is the internal gradient and $B \subset E$ is a structuring element.

The edges that result from these operators are the supremum of the largest edges for each band. Therefore, the segmentation from these gradients can give poor results if the color image is too noisy.

The next two definitions treat color pixel values as vectors in the color space.

Definition 3.5 Let L be a lattice as defined in section 2, the norm, or distance III of a color $l \in L$ is given by:

$$d_{III}(l) = \lfloor (l_1^2 + l_2^2 + l_3^2)^{\frac{1}{2}} \rfloor. \quad (5)$$

where $\lfloor p \rfloor$ means the floor of the value of p [7].

Definition 3.6 Let L be a lattice as defined in section 2, the color distance IV between l and l' ($l, l' \in L$) is given by:

$$d_{IV}(l, l') = \bigvee \{|l_1 - l'_1|, |l_2 - l'_2|, |l_3 - l'_3|\}. \quad (6)$$

The next two gradients are based on the norm and on color distances.

Definition 3.7 Given $f \in Fun[E, L]$, the color gradient III of f , $\nabla_B^{III}(f)$, is given by:

$$\nabla_B^{III}(f)(x) = d_{III}(u), \quad (7)$$

where $u = (f_1(y_M) - f_1(y_m), f_2(y_M) - f_2(y_m), f_3(y_M) - f_3(y_m))$, y_M is the point such that $d_{III}(f(y_M)) = \bigvee_{y \in B_x} d_{III}(f(y))$, y_m is the point such that $d_{III}(f(y_m)) = \bigwedge_{y \in B_x} d_{III}(f(y))$ and $B \subset E$ is a structuring element centered at the origin of E .

Definition 3.8 Given $f \in Fun[E, L]$, the color gradient IV of f , $\nabla_B^{IV}(f)$, is given by:

$$\nabla_B^{IV}(f)(x) = \bigvee_{y \in B_x} d_{IV}(f(x), f(y)), \quad (8)$$

where $B \subset E$ is a structuring element centered at the origin of E .

The next definition is useful for gradients computed under IHS color system. Since intensity and saturation are represented by functions $g \in Fun[E, K]$, their gradients can be computed by $\nabla_B(\bullet)$. However, this is not the case for hue, whose representation is given by a function $h \in Fun[E, \Theta]$. In order to compute a gradient for hue, it is necessary to define a metric function for it.

Definition 3.9 Let $\theta_1, \theta_2 \in \Theta$. The hue distance between θ_1 and θ_2 is given by:

$$d_h(\theta_1, \theta_2) = \lfloor \wedge \{|\theta_1 - \theta_2|, 360 - |\theta_1 - \theta_2|\} \rfloor. \quad (9)$$

The distance introduced above returns an integer value between 0 and 180. In order to compute the proposed gradient, these values will be normalized to K . Let $m_K : [0, 180] \rightarrow [0, k - 1]$ be the normalization function.

Definition 3.10 Given an image $h \in Fun[E, \Theta]$, the angular gradient $\nabla_\Theta(h)$, $\nabla_\Theta : Fun[E, \Theta] \rightarrow Fun[E, K]$, is given by, for all $x \in E$,

$$\nabla_\Theta(h)(x) = m_K \left(\bigvee_{y \in \{B_x - \{x\}\}} d_h(h(x), h(y)) - \bigwedge_{y \in \{B_x - \{x\}\}} d_h(h(x), h(y)) \right). \quad (10)$$

where $B \subset E$ is a structuring element centered at the origin of E .

Let μ_a , μ_b and μ_c be three integers. The following gradient is defined as a linear combination of the morphological gradients for I and S with the angular gradient for H . The coefficients of the linear combination are used to enhance or to obscure the peaks of a gradient image.

Definition 3.11 Given $f \in Fun[E, L]$ in the IHS color model. The color gradient V , $\nabla^V(f)$, $\nabla^V : Fun[E, L] \rightarrow Fun[E, \mathbf{Z}]$, is defined by:

$$\nabla^V(f) = \mu_a \nabla_B(f_1) + \mu_b \nabla_\Theta(f_2) + \mu_c \nabla_B(f_3), \quad (11)$$

where f_1 , f_2 and f_3 represent respectively the I , H , S color bands and $B \subset E$ is a structuring element centered at the origin of E .

The color gradient introduced above is called *sum of weighted gradients* because each gradient is scaled in order

to improve or decrease the weight in the sum. For example, on images where the hue information is the most important, the hue gradient could give a good result by itself. However, in some cases it is not sufficient to enhance the border between objects with similar hues; it could be necessary to weight, for example, the saturation gradient in order to distinguish the borders. The linear combination of gradients to enhance edges on color images is also valid and should be tested under other color models.

Transforming the coordinates from RGB to YIQ and taking only the Y component of the image (which holds the graylevel information) one can use the morphological gradient on this band to define another gradient.

Definition 3.12 Given an image $f \in Fun[E, L]$ in the YIQ color model, the gradient $\nabla^{VI}, \nabla^{VI} : Fun[E, L] \rightarrow Fun[E, K]$, of f is given by:

$$\nabla^{VI}(f) = \nabla_B(f_1) \quad (12)$$

where $B \subset E$ is a structuring element centered at the origin of E .

4 Beucher-Meyer Paradigm

Image segmentation in the context of Mathematical Morphology is usually done by a powerful segmentation method that finds exact borders of specified objects. This method simplifies the segmentation process reducing the problem of segmenting objects directly to the problem of finding markers for the specified objects [8, 9].

Finding the borders of the objects one wants to segment using the watershed operator [10, 11, 12] is the base of the paradigm. In order to select the desired borders and to avoid the known over-segmentation effects [8, 12], a previous preprocessing based on connected filters [13] (which do not deform the borders) is usually applied.

Borders of colored objects are discontinuities between neighbor pixels in the color space. These borders can be detected using the color gradients presented above. As the graylevel gradient, they are also very sensitive to noise in the image, i.e., they enhance the transitions due to the borders of the objects and also the transitions due to noise. Therefore the gradient image is usually a noisy image in the sense that it carries more information than it is necessary. The consequence is that the result of the watershed operator to the gradient image is usually over-segmented [12, 9, 14]. The solution is already classical: to eliminate the borders one does not want by applying an operator that changes the homotopy [1] of the gradient function [8, 9, 14].

Given an image f , the homotopy operator, is a filter [1, 15, 14] that changes only the regional minima [16, 1, 15] of f (there is no modification on the regional maxima [16, 1, 15]). Hence, one can say that it changes the

homotopy tree of f because it changes the low homotopy of f [16]. This property is important because it guarantees that the watershed lines found in the filtered image are a subset of the watershed lines found in the gradient image, i.e., no regional maximum is added, only regional minima are suppressed.

After the application of that filter on the gradient image, the watershed operator finds only the borders of the objects one wants to segment. This method is known as “Beucher-Meyer paradigm” [8].

5 Experimental Results

In this section, we discuss the application of Beucher-Meyer paradigm using the gradients presented in Section 3. Several experiments are shown with various color images in order to compare the effects of the gradients in the result of the segmentation. The quality of each experiment is quantified visually following two criteria: (a) how much the watershed lines extends away from the object borders, and (b) how much the watershed lines are contained in the object to be segmented, i.e, the object is not entirely segmented.

The goal in the first experiment is to segment the red ball (Fig. 1a). An inside marker is assigned to this ball, as well as, an external marker (Fig. 1b) which are used to apply the paradigm. There are several colored balls in the image and the borders of the balls will be enhanced distinctly for each gradient as the experiments show. For all the following experiments, Gradients I, II and III are applied on RGB images; Gradients IV and V are applied on IHS images; and Gradient VI is applied on YIQ images.

Gradient I (Fig. 2a) provides a good border enhancement, but in some cases it misses some important borders. The resulting segmentation (Fig. 2b) is an example where part of the correct border is misplaced (it segments part of the orange ball).

Gradient II (Fig. 2c) is better than I but the result of the segmentation (Fig. 2d) is still wrong in the sense that the watershed line is larger than the ball.

Gradient III (Fig. 2e) is better than II but some small shadows still appear (Fig. 2f).

The same problem reported with gradient I happens with gradients IV and V (Fig. 2g and Fig. 2i). For gradient V, when the same weight, $\mu_a = \mu_b = \mu_c = 1$, is given for each gradient, the information of each gradient is not sufficient to enhance a border between the red and the orange ball (Fig. 2i) and these objects are segmented as one (Fig. 2j). This occurs because the hue information is the most important in the process of segmenting the red ball for this image but the red and the orange balls have similar hues.

The resulting segmentation using gradient V can be fixed by a weight adjustment in the saturation ($\mu_c = 10$

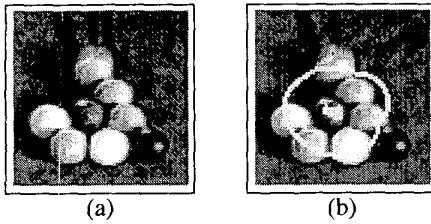


Figure 1: (a) Original image. (b) Markers.

and $\mu_a = \mu_b = 1$). Figure 2k shows the gradient V with the new weighting. The result of the segmentation after this weighting is shown in Fig. 2l. Notice the border between the red and the orange balls.

Gradient VI (Fig. 2m) gives a good result but, as I, II and III, some small shadows still appear (Fig. 2n).

Figure 3a shows another image for which the experiment is repeated. There is only one ball, but the image has some interesting characteristics. Besides the existence of two shady regions, the image is blurred. Again, the internal and external markers are provided (Figure 3b).

All color gradients enhance well the borders (Fig. 4a, c, e, g, i, k, m) and their respective segmentations (Fig. 4 b, d, f, h, j, l, n) are good, despite the location of the ball around a blurred region with high luminosity. Visually, gradient V with the same weight $\mu_a = \mu_b = \mu_c = 1$ for all the bands (Fig. 3i) and with weighting $\mu_c = 10$ and $\mu_a = \mu_b = 1$, as before (Fig. 3k), are the ones that better enhance the border of the red ball (Fig. 3j and Fig. 3l, respectively). This last is visually almost perfect. For thirty three different images similar to these two presented, gradient V makes very few mistakes in relation to the others.

The last experiment we show is done with an image of better visual quality. Figure 5 shows an image of colored jelly beans and Fig. 6 shows the markers used to segment the green beans.

Figures 7, 8, 9, 10, 11, 12 and 13 show the result of the segmentation when gradients I, II, III, IV, V with same weights ($\mu_a = \mu_b = \mu_c = 1$), V with weights $\mu_a = 0$, $\mu_b = 1$ and $\mu_c = 0$, and VI, respectively, are applied. All segmentations apparently have errors but gradient V with weights $\mu_a = 0$, $\mu_b = 1$ and $\mu_c = 0$ is the most coherent because there are green beans below the marked ones, that are segmented together, giving the impression that the segmentation is wrong. Actually, there are fewer markers than necessary.

6 Conclusion

The color image segmentation problems can be solved by Beucher-Meyer paradigm if we use a suitable color metric to define a color gradient. Several color gradients have been defined and tested in conjunction with the paradigm. The

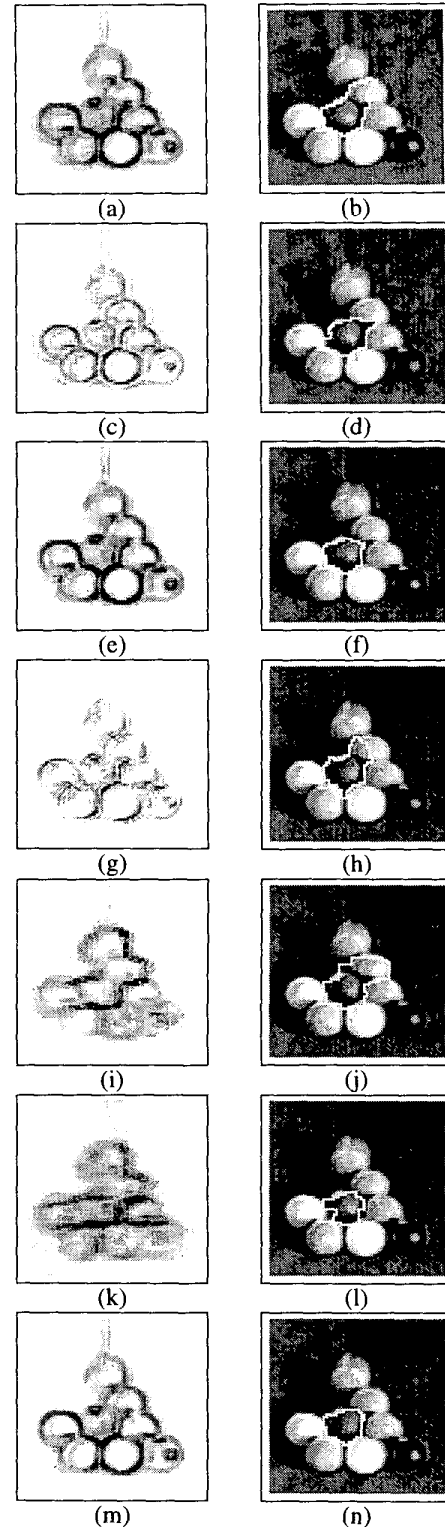


Figure 2: Color gradient and watershed lines. (a-b) gradient I. (c-d) gradient II. (e-f) gradient III. (g-h) gradient IV. (i-j) gradient V. (k-l) gradient V (weighted). (m-n) gradient VI.

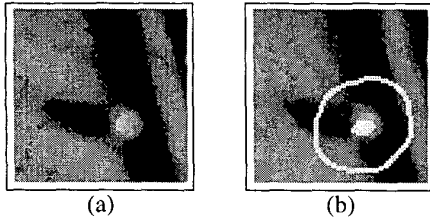


Figure 3: Another example of markers (a) Original image. (b) Markers.

weighted gradient (gradient V) visually gives the best results but some more experiments have to be done. The major difficult with the weighted gradient is to find the correct weights. For this problem we still do not have a systematic solution.

7 Acknowledgments

The first author acknowledges support from CNPq (process 571279/1997-0), the second author acknowledges support from FAPESP (process 98/00311-4). The authors also acknowledge Rafael Santos for the use of the Color toolbox for Khoros.

References

- [1] J. Serra. *Image Analysis and Mathematical Morphology*. Academic Press, 1982.
- [2] H. J. A. M. Heijmans. *Morphological Image Operators*. Academic Press, Boston, 1994.
- [3] H. Talbot, C. Evans, and R. Jones. Complete Ordering and Multivariate Mathematical Morphology: Algorithms and Applications. In Henk J.A.M. Heijmans and Jos B.T.M. Roerdink, editors, *Mathematical Morphology and its Applications to Image and Signal Processing*, volume 12 of *Computational Imaging and Vision*, pages 27–34. Kluwer Academic Publishers, Dordrecht, May 1998.
- [4] J. Chanussot and P. Lambert. Total Ordering Based on Space Filling Curves for Multivalued Morphology. In Henk J.A.M. Heijmans and Jos B.T.M. Roerdink, editors, *Mathematical Morphology and its Applications to Image and Signal Processing*, volume 12 of *Computational Imaging and Vision*, pages 51–58. Kluwer Academic Publishers, Dordrecht, May 1998.
- [5] E. R. Dougherty, editor. *Digital Image Processing Methods*. Marcel Dekker, 1994.
- [6] W. K. Pratt. *Digital Image Processing*. John Wiley and Sons, 1991.

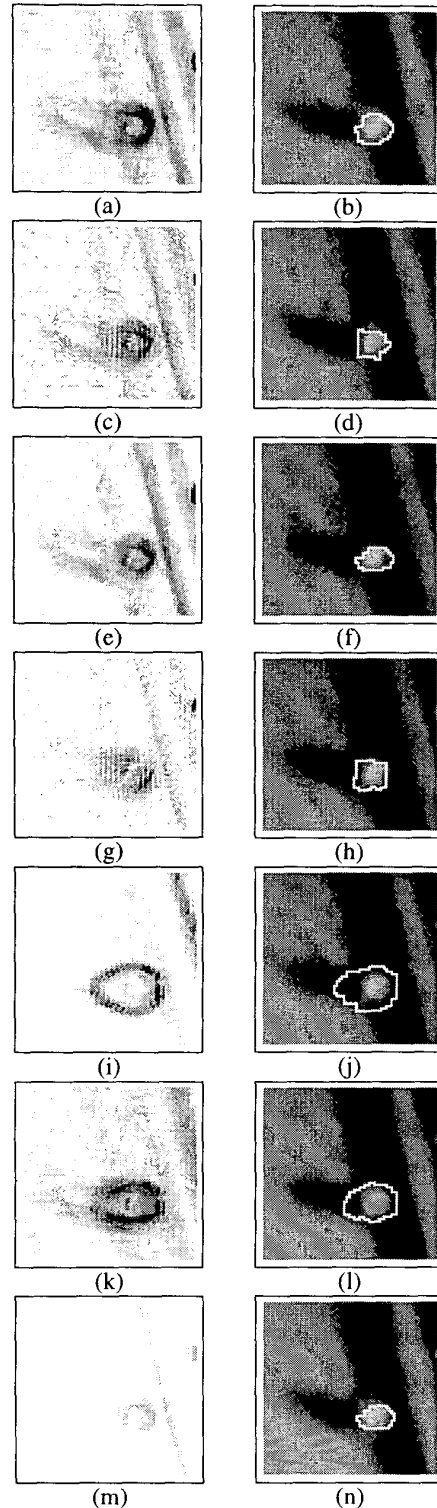


Figure 4: Color gradient and watershed lines. (a-b) gradient I. (c-d) gradient II. (e-f) gradient III. (g-h) gradient IV. (i-j) gradient V. (k-l) gradient V (weighted). (m-n) gradient VI.

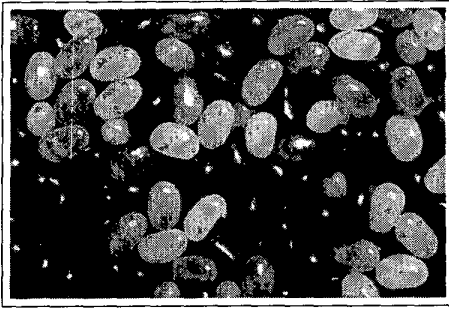


Figure 5: Original JellyBeans image.

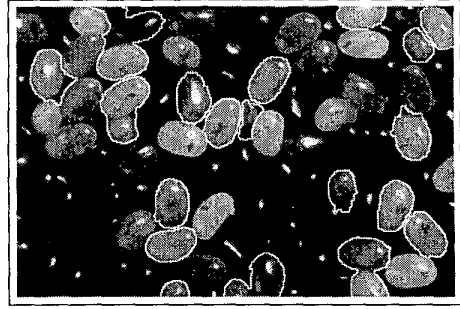


Figure 9: Gradient III.

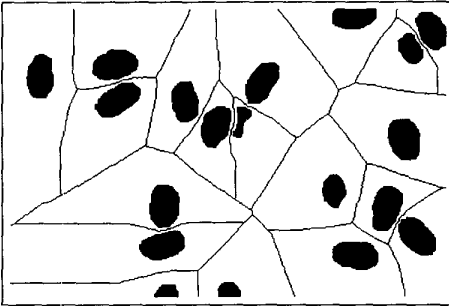


Figure 6: Markers for the green beans.

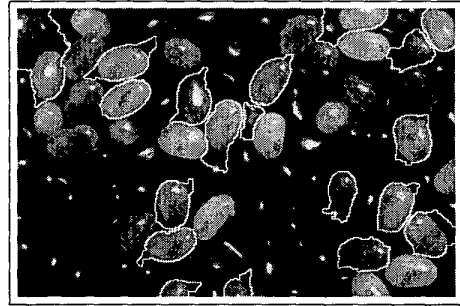


Figure 10: Gradient IV.

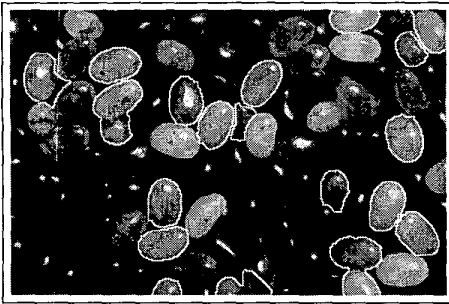


Figure 7: Gradient I.

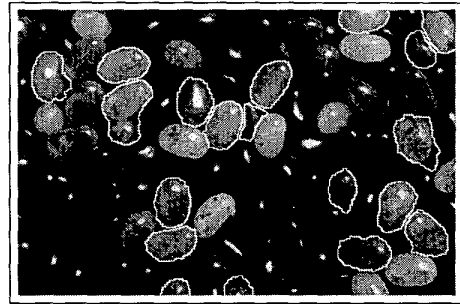


Figure 11: Gradient V.

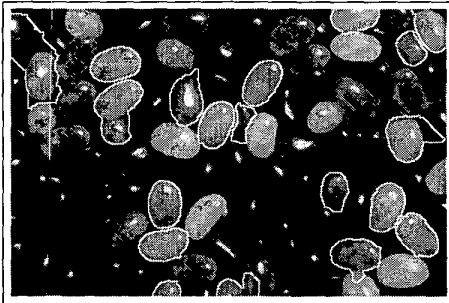


Figure 8: Gradient II.

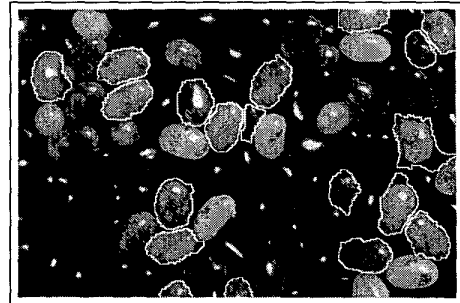


Figure 12: Gradient V - weighted.



Figure 13: Gradient VI.

[16] F. Meyer. Skeletons and Perceptual Graphs. *Signal Processing*, 16:335–363, 1989.

- [7] T. H. Cormen, C. E. Leiserson, and R. L. Rivest. *Introduction to Algorithms*. McGraw-Hill, 1990.
- [8] F. Meyer and S. Beucher. Morphological Segmentation. *Journal of Visual Communication and Image Representation*, 1(1):21–46, September 1990.
- [9] R. Hirata Jr. Segmentação de Imagens por Morfologia Matemática. Master's thesis, Instituto de Matemática e Estatística - USP, março 1997.
- [10] S. Beucher. Watersheds of Functions and Picture Segmentation. In *ICASSP 82, Proc. IEEE Intern. Conf. on Acoustics, Speech and Signal Processing*, pages 1928–1931, Paris, May 1982.
- [11] P. Soille and L. Vincent. Determining Watersheds in Digital Pictures via Flooding Simulations. In *Visual Communications and Image Processing*, pages 240–250. SPIE, 1990. volume 1360.
- [12] L. Vincent and P. Soille. Watersheds in Digital Spaces: An Efficient Algorithm Based on Immersion Simulations. *IEEE Transactions on Pattern Analysis and Machine Intelligence*, 13(6):583–598, June 1991.
- [13] H. J. A. M. Heijmans. Introduction to Connected Operators. In E. R. Dougherty and J. T. Astola, editors, *Nonlinear Filters for Image Processing*, pages 207–235. SPIE–The International Society for Optical Engineering, 1999.
- [14] R. Hirata Jr., J. Barrera, F. C. Flores, and R. A. Lotufo. Automatic Design of Morphological Operators for Motion Segmentation. In J. Stolfi and C. L. Tozzi, editors, *Proc. of Sibgrapi'99*, pages 283–292, Campinas, SP, Brazil, 1999.
- [15] J. Serra. *Image Analysis and Mathematical Morphology. Volume 2: Theoretical Advances*. Academic Press, 1988.